

Evolution of Crystalline Structures of Poly(ϵ -caprolactone)/Polycarbonate Blends. 1. Isothermal Crystallization Kinetics As Probed by Synchrotron Small-Angle X-ray Scattering

Y. Wilson Cheung^{*,†} and Richard S. Stein^{*}

Department of Polymer Science and Engineering, University of Massachusetts, Amherst, Massachusetts 01003

Benjamin Chu and Guangwei Wu

Department of Chemistry, State University of New York at Stony Brook, Long Island, New York 11794-3400

Received October 7, 1993; Revised Manuscript Received April 5, 1994[®]

ABSTRACT: Evolution of the poly(ϵ -caprolactone) (PCL) lamellae in blends of PCL/PC (polycarbonate) was monitored by synchrotron small-angle X-ray scattering (SAXS). The effects of crystallization temperature, PC concentration, and PC crystallinity on the PCL lamellar growth in the PCL-rich blends were investigated. The half-crystallization time derived from the temporal change of the peak intensity increased with crystallization temperature and generally increased with the addition of PC. For a given blend composition, the lamellar growth rate increased with increasing PC crystallinity. The interlamellar spacing initially varied with time and then approached a plateau value at the later stage of crystallization. An insertion mechanism is proposed in which the PCL is crystallized in the amorphous intralamellar phase. This model is also consistent with the quantitative SAXS results,⁶ which suggested that random mixing of PCL and PC lamellae occurred in the semicrystalline (PCL)/semicrystalline (PC) state.

Introduction

The phase behavior of poly(ϵ -caprolactone) (PCL)/polycarbonate (PC) blends is extremely rich and enormously complicated. On the basis of thermal analysis measurements, the PCL/PC blends are miscible in the amorphous phase, as demonstrated by a single glass transition temperature, over the entire composition range.¹⁻⁴ This blend system exhibits a multitude of phase transitions and very complex morphologies.^{5,6} For the PCL-rich blends, both PCL and PC readily crystallize at room temperature and hence these materials are classified as semicrystalline/semicrystalline blends. Above the melting point of PCL ($\sim 60^\circ\text{C}$), the blends become amorphous/semicrystalline. The PCL-rich blends turn completely amorphous at temperatures above the melting transition of PC ($\sim 230^\circ\text{C}$). Phase separation occurs at the lower critical solution temperature (LCST $\sim 260^\circ\text{C}$) where PCL and PC undergo demixing. Due to the thermal instability of PCL at these elevated temperatures, the blends may further undergo thermal degradation and/or trans-esterification as evidenced by the evolution of carbon dioxide.¹

Unique to the PCL-rich blends is the three-phase structure in which two distinctly different crystalline phases coexist with a mixed amorphous phase as revealed by thermal analysis and wide-angle X-ray scattering.¹⁻³ The semicrystalline/semicrystalline nature of this blend system offers an unique window through which one can study the effects of crystallinity of one component on the crystallization kinetics of the other component. Since both the glass transition temperatures (T_g) and the melting points (T_m) of PCL and PC are widely separated, the crystallization windows for these polymers are consequently very different.

This comprehensive study is one of the first attempts at unraveling the complex crystallization mechanism of a

semicrystalline/semicrystalline blend system at both the microscopic and macroscopic levels. In the second part of this series of investigations,⁷ the crystallization kinetics of PCL in the PCL-rich blends will be examined by differential scanning calorimetry and optical microscopy. These thermal and optical measurements yield information on the overall crystallization rate and the radial growth rate, respectively. On the basis of these results, the composite effects of nucleation and growth can be decoupled and analyzed with the nucleation and growth theory. In addition to the traditional variables of composition and crystallization temperature, the effects of PC crystallinity on the PCL crystallization kinetics will be explored.

In order to probe the crystallization kinetics at a microscopic level, time-resolved synchrotron small-angle X-ray scattering (SAXS) was employed to monitor the PCL lamellar evolution in the PCL-rich blends. This paper will focus on the isothermal crystallization kinetics of PCL in the PCL-rich blends containing various amounts of PC crystallinity. The effects of crystallization temperature and PC composition will also be examined. There are three basic parameters which could be easily obtained from synchrotron SAXS. Lamellar development is normally described in terms of the time evolution of the long period as measured by the peak position of the scattering profile. It has been observed that the long period increased with time for polyethylene,⁸ decreased for poly(ethylene terephthalate) (PET),⁹ and remained constant for poly(β -hydroxybutyrate).¹⁰ The changes in the long period during the course of crystallization are usually related to lamellar reorganization as the lamellae may undergo isothermal thickening or flattening. The nature and magnitude of these lamellar rearrangements are not well understood. The second parameter is the intensity of the peak, which reflects the growth of the crystalline phase. The third parameter is the invariant, which is proportional to the product of the volume fractions of the two phases and the electron density difference between the crystal and the amorphous region and is often used as a measure of crystallinity.

[†] Present address: Dow Chemical Company, Midland, MI 48674.

[®] Abstract published in *Advance ACS Abstracts*, May 15, 1994.

Table 1. Molecular Weights for Poly(ϵ -Caprolactone) (PCL) and Polycarbonate (PC)

polymer	M_w	M_n	M_w/M_n
PCL	23,700	16,500	1.44
PC	23,100	36,400	1.57

Dynamic studies¹¹ of isothermal crystallization kinetics of PCL and 90% PCL/10% poly(vinyl chloride) (PVC) blend by synchrotron SAXS indicated that the long period for both the pure PCL and the blend remained virtually constant with time. Kinetic parameters such as the half-crystallization time $\tau_{1/2}$ and the Avrami exponent n were derived from the time dependence of the peak intensity. The blend showed a higher $\tau_{1/2}$ than that for the pure PCL for a given crystallization temperature. Similar to this behavior, the PCL crystallization rate for the PCL/PC blends is slower than that for the pure PCL. The degree of PC crystallinity is expected to have a profound impact on the lamellar development. The focus of this study will be directed at elucidating the effects of crystalline PC on the lamellar evolution and structure of PCL in the PCL-rich blends.

Experimental Section

Both PCL and PC were obtained from Scientific Polymer Products and their molecular weights are shown in Table 1. The two homopolymers were dissolved and mixed in chloroform, yielding a 5 wt % solution. The blends were subsequently recovered from solution by precipitating them in methanol. The blends were first air dried overnight and then vacuum dried at 90 °C for 2 days. Similar purification procedures and thermal treatments were applied to the pure PCL. As-precipitated (AP) blends were used for the study after vacuum drying without any further thermal treatments. Quenched (Q) blends were prepared by first heating the AP blends to 250 °C (above the melting point of PC) for 3 min and then quenching them to room temperature.

Thermal transitions were measured with a Dupont-10 differential scanning calorimeter (DSC) at a heating rate of 20 °C/min. Melting points were recorded from the peak temperatures of the melting endotherms measured from the first heating scan. On the basis of the values for the heat of fusion for 100% crystalline PC¹² (35.3 cal/g) and PCL¹³ (32.4 cal/g), the degree of crystallinity of both PCL and PC was calculated from the melting endotherm and normalized with respect to the composition of each component in the blend.

The scattering samples were deposited into a copper cell contained between two 25- μ m-thick Kapton films. The sample dimension was about 7 mm in diameter and 2 mm in thickness. Synchrotron SAXS measurements were performed on the State University of New York (SUNY) X3A2 Beamline, National Synchrotron Light Source (NSLS), Brookhaven National Laboratories (BNL), using a modified Kratky block collimation system.¹⁴ The storage ring of the synchrotron was operated at an energy level of 2.6 GeV with a beam current of 110–180 mA. The X-ray wavelength used for the measurement was 1.54-Å. The scattered intensity was collected by a linear position sensitive photodiode array detector coupled to an optical multichannel analyzer.¹⁴ The scattering profiles were corrected for detector nonuniformity, sample absorption, background, and incident X-ray intensity fluctuations.^{15,16}

Temperature quenching experiments were conducted in a device consisting of two thermal chambers equilibrated at temperatures T_C and T_H .¹⁷ The sample cell could be transferred rapidly from one chamber to the other chamber by means of a metal rod connected to a pneumatic pressure device. Isothermal crystallization was achieved by preheating the sample at 75 °C in the T_H chamber for about 5 min in order to render PCL completely amorphous and then rapidly transferred to the T_C chamber equilibrated at the crystallization temperature. Since the thermal chambers were well insulated and the temperature jump was fairly shallow (~ 30 °C), it was estimated that the sample reached the crystallization temperature in about a minute. This time scale was generally shorter than the induction time for PCL

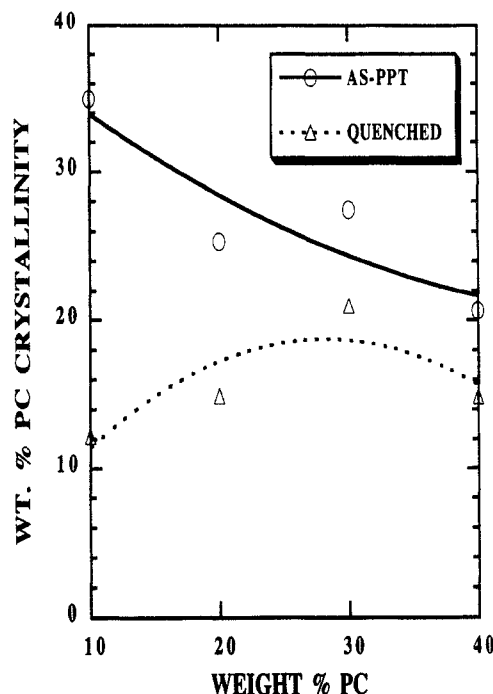


Figure 1. Normalized wt % PC crystallinity for as-precipitated (AP) and quenched (Q) blends. The lines are drawn only for guiding the eyes.

crystallization. The scattered intensity during the crystallization was recorded every 10–50 s until the integrated intensity ceased to change. The temperature fluctuation in the chamber was within ± 0.3 °C during the course of the measurement.

Results and Discussion

The degree of PC crystallinity in the PCL-rich blends is dependent on the sample preparation and thermal history. As described earlier, the Q blends were prepared by heating the AP samples to 250 °C for 3 min to destroy PC crystallinity and then quenching them to room temperature. Effectively, the PC crystallinity developed represented the “quasi-equilibrium” crystallinity attained at room temperature. In contrast, the AP blends were recovered from precipitation with methanol and were vacuum dried at 90 °C for 2 days. These blends were used for the study without further thermal treatments. Due to the annealing effects from drying, the AP blends invariably have higher PC crystallinity than the corresponding Q blends, as shown in Figure 1. The isothermal crystallization kinetics for the pure PCL, Q blends, and AP blends will be discussed and compared below.

I. Pure PCL. The time evolution of $q^2 I(q)$ for pure PCL crystallized at 41 °C as measured by synchrotron SAXS is shown in Figure 2. The integrated SAXS intensity or the invariant $Q(t)$ for a two-phase system with sharp interface boundaries is defined as¹⁸

$$Q = \int_0^\infty q^2 I(q) dq \propto \phi_c (1 - \phi_c) (\rho_c - \rho_a)^2 \quad (1)$$

where ρ_a and ρ_c are, respectively, the electron densities of the amorphous and the crystalline phases, ϕ_c is the degree of crystallinity, and $q = (4\pi \sin(\theta/\lambda))$, with 2θ being the scattering angle and λ the X-ray wavelength. On the basis of this equation, the invariant attains a maximum at 50 volume % of crystallinity and could be used as a measure of crystallinity. The normalized invariant, $Q(t)/Q_{\max}$, as shown in Figure 3, revealed a maximum indicating that the degree of crystallinity had exceeded the 50% value. The interlamellar spacing and the peak intensity I_{\max} are

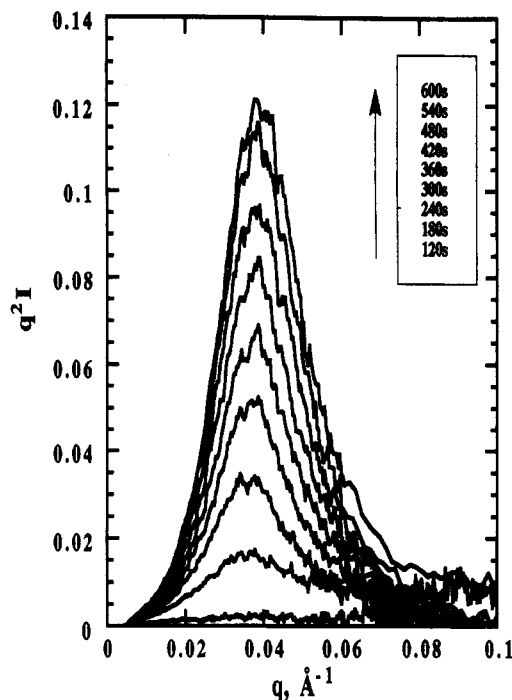


Figure 2. Synchrotron SAXS profiles for PCL crystallized at 41 °C. Crystallization time measured in seconds is indicated in the legend. Each SAXS profile was accumulated for 20 s.

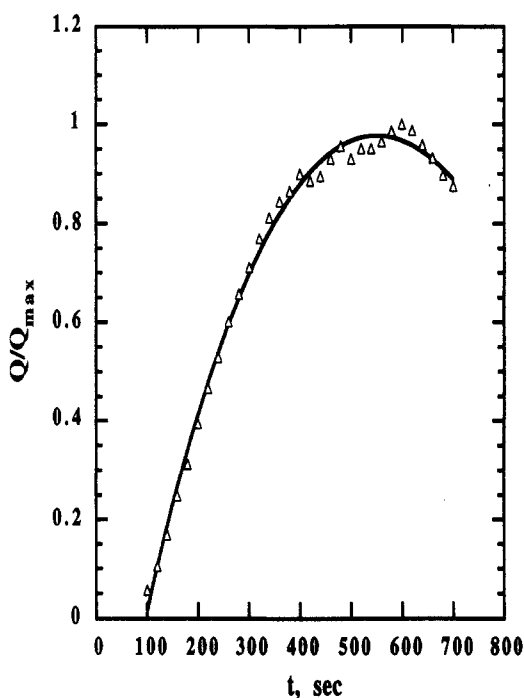


Figure 3. Normalized invariant for pure PCL crystallized at 41 °C.

shown in Figure 4. The PCL interlamellar spacing remained fairly constant during the course of crystallization, in agreement with other studies.¹¹ Similar to the invariant, the peak intensity exhibited a sigmoidal time dependence reflecting the development of crystallinity. Therefore, both the normalized invariant and the peak intensity could be used to monitor the crystallization process.

II. Quenched Blends. A series of Lorentz-corrected SAXS profiles for an 80% PCL/20% PC Q blend also crystallized at 41 °C is shown in Figure 5. Two striking features were readily observed from these SAXS profiles. First, there was finite scattering at time zero, indicating preexisting structure. Second, the peak position changed

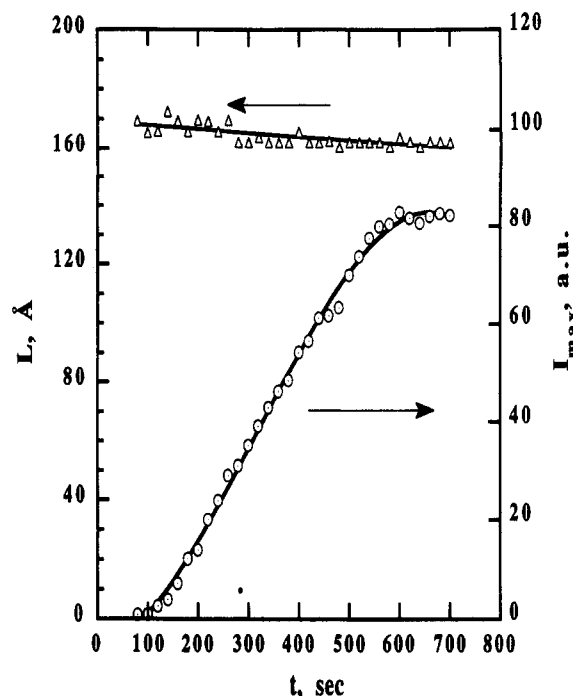


Figure 4. Time dependence of the long period, L , and the peak intensity, I_{\max} , for pure PCL crystallized at 41 °C. The triangles represent the long period and the circle denotes the I_{\max} .

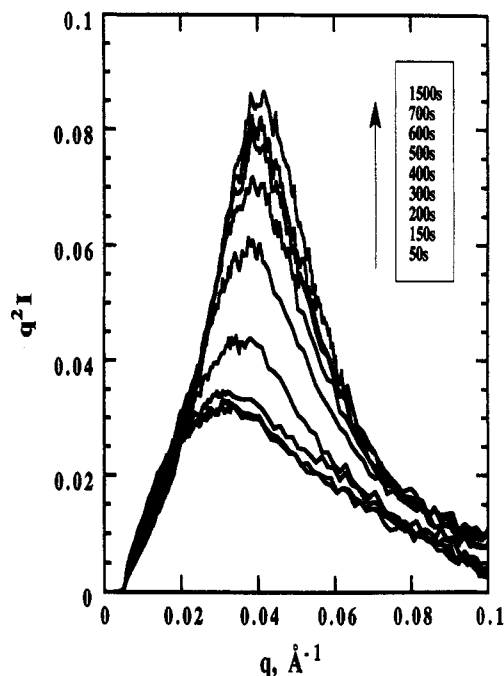


Figure 5. Synchrotron SAXS profiles for an 80% PCL/20% PC quenched blend crystallized at 41 °C. Crystallization time measured in seconds is indicated in the legend. Each SAXS profile was accumulated for 50 s.

with time, reflecting some kind of lamellar rearrangement. Figures 6 illustrates these two unusual behaviors. The excess scattering mainly came from the PC lamellae in the blends. As PCL was being crystallized, the long period initially decreased with time and finally approached a plateau value as indicated by Figure 6. Similar patterns were observed in other quenched blends crystallized at various temperatures.

A series of crystallization isotherms (I_{\max} versus time) for blends crystallized at 37 °C is plotted in Figure 7. A cursory examination of these plots revealed that the scattering at time zero increased with increasing PC whereas the magnitude of the change in peak scattering

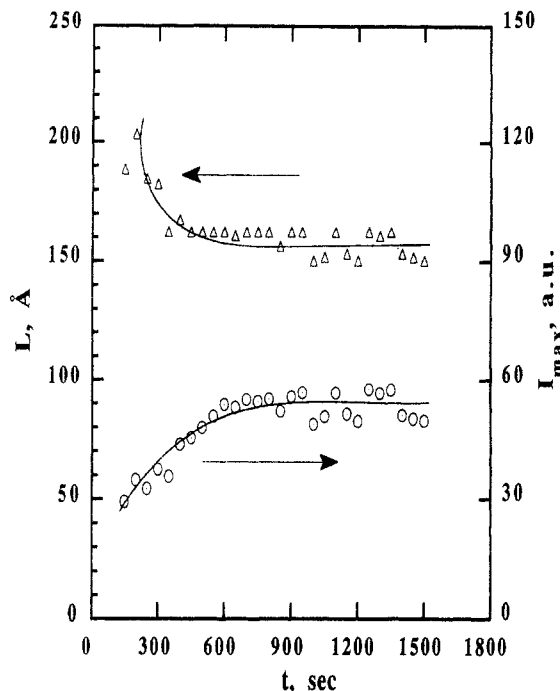


Figure 6. Time evolution of the long period, L , and the peak intensity, I_{\max} , for an 80% PCL/20% PC quenched blend crystallized at 41 °C. The triangles represent the long period and the circles denote the I_{\max} .

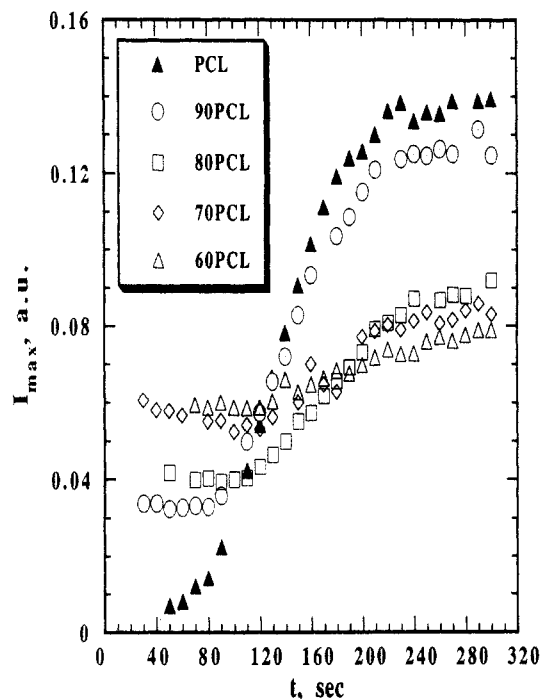


Figure 7. Crystallization isotherms for the quenched blends crystallized at 37 °C.

intensity, as measured by $[I_{\max}(\infty) - I_{\max}(0)]$, decreased with increasing PC. It is clearly observed that the excess scattering generally increased with increasing PC crystallinity and predominantly came from the PC lamellae. The reduction in the magnitude of the change in the peak scattering intensity reflected a corresponding decrease in the PCL crystallinity. The half-crystallization times, $\tau_{1/2}$, defined as the time required to achieve 50% of the normalized crystallinity measured in terms of the change in the peak scattering intensity, as a function of the PC composition and crystallization temperature are shown in Figure 8. Similar to the overall crystallization rate results,⁷ $\tau_{1/2}$ increased with crystallization temperature and gener-

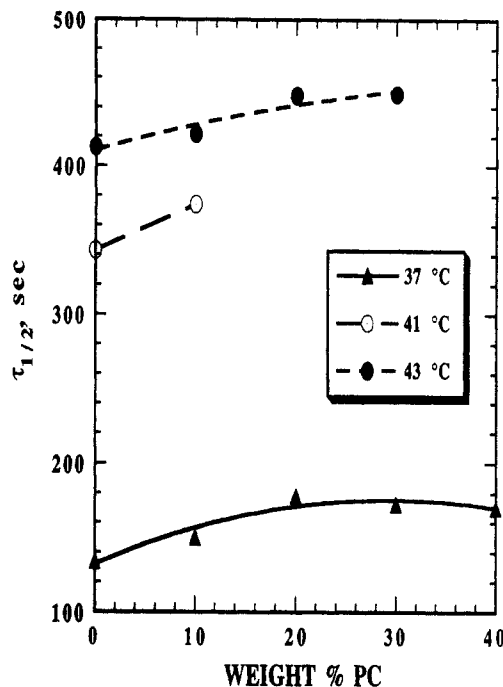


Figure 8. Half-crystallization times, $\tau_{1/2}$, for the quenched blends.

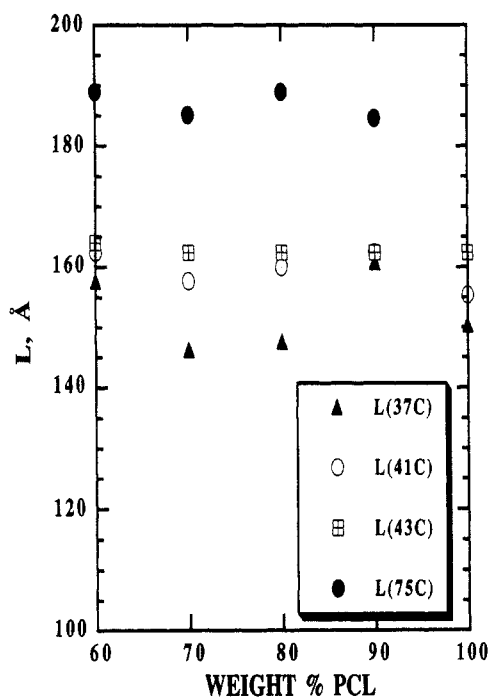


Figure 9. Long period as a function of crystallization temperature and composition for the quenched blends.

ally increased with the addition of PC. Invariably, the value of the half-crystallization time derived from synchrotron SAXS was always larger than that obtained from DSC. On the basis of the DSC results coupled with the present findings, it was found that there exists a very strong parallel between the overall rate of crystallization and the lamellar growth as the kinetics for these two processes are comparable.

The composition and crystallization temperature dependence of the "equilibrium" long period, obtained at the end of the crystallization, are summarized in Figure 9. Due to the difference in the degree of undercooling, the long period increased with the crystallization temperature. Furthermore, the long period remained fairly independent of the PC composition. Additionally, the long periods

obtained at 75 °C are somewhat larger than those measured at lower temperatures. The scattering at 75 °C arose mainly from PC as the PCL ($T_m \sim 60$ °C) became amorphous at this temperature. Hence, the long periods measured at 75 °C represented the actual interlamellar spacing for PC. These values were similar to those measured during the induction period of the PCL crystallization. It was found that the actual PCL long period could not be isolated as the SAXS measured at various crystallization temperatures (below the T_m of PCL) came from a superposition of the PC and PCL lamellar scattering. Effectively, the long period derived at temperatures below the T_m of PCL could be viewed as the average long period for the PC and PCL lamellae. Careful analysis of the composition dependence of the peak width and interfacial thickness⁶ provided strong evidence that the PCL and PC lamellae are randomly mixed in the semicrystalline/semicrystalline state.

As discussed earlier, the time dependence of the long period reflects the lamellar organization during the crystallization. For all the blends investigated, the long period initially decreased with time and then approached a plateau value characteristic of the average interlamellar spacing for the PC and PCL lamellae. On the basis of these findings, an insertion mechanism is proposed in which the PCL is crystallized in the amorphous intralamellar region. According to this insertion model, the new PCL lamellae are formed in the amorphous phase between the existing PC lamellae. This model can easily account for the initial reduction in the long period and the absence of multiple peaks. It is also consistent with the results derived from the quantitative SAXS studies of the PCL-rich blends in the semicrystalline/semicrystalline state, which suggested a random mixing of PCL and PC lamellae.⁶ In other words, PCL and PC lamellae are randomly dispersed in the amorphous phase and the SAXS profiles measured in the semicrystalline/semicrystalline state could be modeled as scattering originating from composite entities consisting of PCL and PC lamellae. The reduction in the PC long period could be attributed to the formation of the PCL lamellae. As crystallization proceeded, the scattering became dominated by the PCL lamellae and the blend long period ceased to change, as was observed for the pure PCL. The "equilibrium" long periods for the blends differed from those of the pure PCL due to the composite nature of the lamellar scattering and the differences in the thermodynamic forces for PCL crystallization arising from blending.

III. As-Precipitated Blends. In addition to the PC composition and crystallization temperature, the effects of PC crystallinity on the PCL lamellar growth were also examined. According to Figure 1, the PC crystallinities for the AP blends were always higher than those for the corresponding Q blends. For a given blend composition, it was found that the AP blends always crystallized faster than the corresponding Q blends, as revealed by DSC.⁷ This difference was attributed to the depletion of PC in the mixed amorphous phase due to crystallization which result in a higher mobility. To a first order of approximation, the PCL crystallization kinetics are governed by the total amount of amorphous PC present in the blends. The PC crystallinity effects on the lamellar development will be discussed with respect to and contrasted against the Q blends.

The evolution of the long period and I_{\max} for an 80% PCL/20% PC blend crystallized at 43 °C is shown in Figure 10. In contrast to the Q blends, the long period for the AP blends initially increased with time and then reached

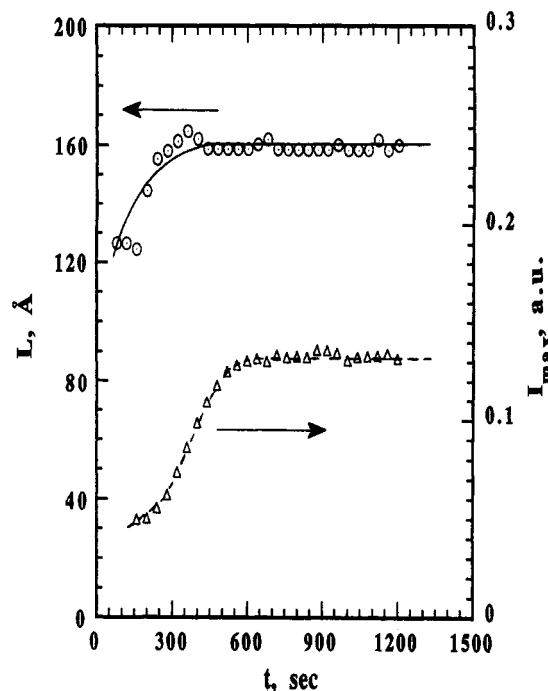


Figure 10. Time evolution of the long period, L , and the peak intensity, I_{\max} , for an 80% PCL/20% PC as-precipitated blend crystallized at 43 °C.

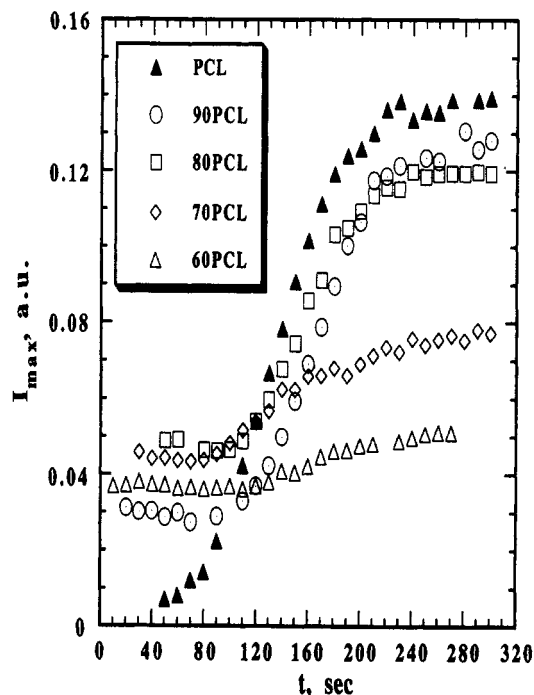


Figure 11. Crystallization isotherms for the as-precipitated blends crystallized at 37 °C.

a plateau value. Similar time dependence was found for other AP blends crystallized at various temperatures. Crystallization isotherms for the AP blends and the pure PCL crystallized at 37 °C are plotted in Figure 11. Nearly identical features to those found in the Q blends are observed. The peak scattering intensity at time zero generally increased with increasing PC crystallinity, whereas the overall change in the peak scattering intensity, $[I_{\max}(\infty) - I_{\max}(0)]$, decreased, reflecting a reduction in the PCL crystallinity, with increasing PC concentration. The half-crystallization time, $\tau_{1/2}$, as a function of PC composition and crystallization temperature is summarized in Figure 12. Similar to the Q blends, the lamellar growth rate decreased with increasing crystallization

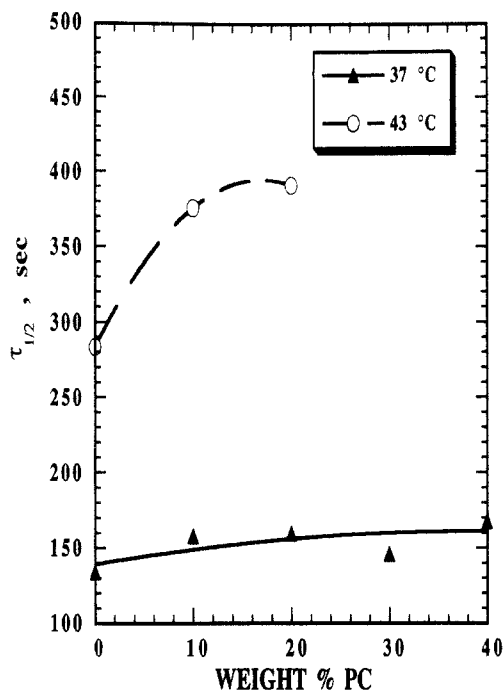


Figure 12. Half-crystallization times, $\tau_{1/2}$, for the as-precipitated blends.

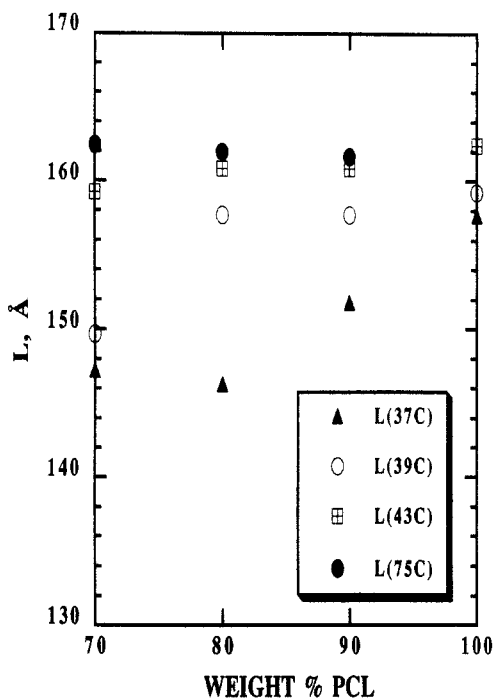


Figure 13. Long period as a function of crystallization temperature and composition for the as-precipitated blends.

temperature and increasing PC. A comparison between Figures 8 and 12 clearly demonstrates that the lamellar growth rate increased with increasing PC crystallinity for a given blend composition. This finding unequivocally shows that the presence of amorphous PC retards both the overall crystallization rate as measured by DSC and the lamellar growth rate as monitored by synchrotron SAXS.

The composition and crystallization temperature dependence of the long period are shown in Figure 13. Similar to the Q blends, a systematic increase in the long period with increasing crystallization temperature was found. The PC long periods (measured at 75 °C) were lower than those obtained for the Q blends. This disparity in the PC lamellar structure might be attributed to the differences

in the thermal history imposed on the samples. The long periods for the AP blends (with smaller PC long periods) were smaller than those found in the corresponding Q blends, thus reflecting the composite nature of the mixed lamellae.

The equilibrium SAXS peak width, as defined by the peak width at half-height, for the AP blends was generally smaller than that for the corresponding Q blends. Additionally, the peak width increased with increasing PCL.⁶ This difference in the heterogeneity of the lamellar sizes could be attributed to the annealing effects resulting from drying at 90 °C. Since the SAXS measured in the semicrystalline/semicrystalline state is a superposition of the PCL and PC lamellar scattering, the narrower peak width found in the AP blends could be a direct result of the narrower PC lamellar distribution resulting from annealing. This finding coupled with the disparity in the long periods between the Q and AP blends provides additional evidence for supporting the random mixing model for PCL and PC lamellae.

One of the most profound differences between the AP and the Q blends could rest with the time evolution of the long period. In contrast to the Q blends, the long period for the AP blends initially increased with time and approached a plateau value in the later stage of crystallization. This behavior suggested that the PC lamellae in the AP blends experienced rearrangement, resulting in a reduction of the long period upon quenching to the PCL crystallization temperature. In the case of the Q blends, the PC lamellae structure remained virtually intact at the PCL crystallization temperature. Several mechanisms could account for the apparent "collapse" of the PC lamellae observed in the AP blends. It is well known that lamellar flattening can lead to a reduction in the long period as the PC may undergo further (secondary) crystallization. Isothermal thinning resulting from low temperature annealing can also account for the decrease in the long period.

The induction period for the AP blends is shorter than that for the Q blends. A recent SAXS study on poly(ethylene terephthalate)¹⁹ revealed that a growth process that is very similar to the spinodal decomposition type of phase separation process occurred during the induction period. Crystallization commences after a dense domain characterized by a long-range ordered structure grows to a certain size. The changes in the PC long period may be related to the scattering arising from this dense domain. As PCL crystallizes, PCL lamellae form in the amorphous intralamellar phase according to the insertion model. Subsequently, these PCL lamellae dominate the scattering, resulting in an invariant in the long period. In agreement with the Q blends, the final crystalline blend morphology is adequately described by the random mixing model in which PCL and PC lamellae are homogeneously dispersed in an amorphous matrix.

The exact origin of the differences observed in the time evolution of the long period between the Q and the AP blends is highly complex and not well understood. However, there are several distinct differences between these two types of blends. Due to the higher PC crystallinity, the mobility in the amorphous phase for the AP blends is higher than that for the corresponding Q blends due to the depletion of PC in the mixed amorphous phase resulting from crystallization. On the basis of the overall crystallization rate results⁷ and the lamellar growth measurements, the AP blends crystallize faster than the corresponding Q blends. As indicated above, the induction period is shorter for the AP blends as compared with that

for the Q blends. It remains a challenge to derive a universal mechanism which can provide a rational explanation for describing the initial time dependence of the long period for the two different blends.

Summary

The isothermal crystallization kinetics of PCL-rich blends containing various amounts of PC crystallinity have been probed with synchrotron SAXS. The effects of PC composition, crystallization temperature, and PC crystallinity on the PCL crystallization kinetics have been systematically investigated. AP blends with higher PC crystallinity were obtained from precipitation followed by vacuum drying and were used without any further thermal treatments. Q blends with lower PC crystallinity were prepared by first heating the AP samples to above T_m of PC and then quenching them to room temperature.

As in the DSC measurements,⁷ the PCL lamellar growth rate for the AP blends was higher than that for the corresponding Q blends. To a first order of approximation, it was found that the crystallization rate was predominantly controlled by the amount of amorphous PC present in the blends. The half-crystallization time derived from the temporal change of the peak intensity increased with the crystallization temperature and generally increased with the addition of PC. Similarly, the long period increased with increasing crystallization temperature.

For the Q blends, the long period initially decreased with time and then reached a plateau value at the later stage of crystallization. An insertion model, where the PCL is crystallized in the amorphous intralamellar phase of the existing crystalline PC, can account for the reduction in the long period and the absence of multiple peaks. This type of crystallization mechanism is also consistent with our quantitative SAXS results,⁶ which suggested that random mixing of PCL and PC lamellae occurred in the semicrystalline/semicrystalline state. In the case of the AP blends, the PC lamellae experienced rearrangement as reflected by the reduction in the long period upon quenching to the PCL crystallization temperature. Additionally, the long period initially increased with time and finally approached a plateau value. The origin of this phenomenon is not well understood and the challenge of

deriving a universal crystallization mechanism which can explain the differences in the time evolution of the lamellae for both the Q and AP blends remains.

Acknowledgment. Support of this work by Novacor Inc. and the Department of Energy (DEFG 0286ER 45237.009) including the use of the SUNY X3A2 Beamline at the National Synchrotron Light Source is gratefully acknowledged. Y. W. Cheung thanks A. Hanyu and M. Sethumadhavan of University of Massachusetts at Amherst for their help with the synchrotron SAXS measurements.

References and Notes

- (1) Cheung, Y. W.; Stein, R. S. *Macromolecules* 1994, 27, 2512.
- (2) Cruz, C. A.; Paul, D. R.; Barlow, J. W. *J. Appl. Polym. Sci.* 1979, 23, 589.
- (3) Jonza, J. M.; Porter, R. S. *Macromolecules* 1986, 19, 1946.
- (4) Coleman, M. M.; Painter, P. C. *J. Appl. Spect. Rev.* 1984, 20(3&4), 255.
- (5) Cheung, Y. W.; Stein, R. S.; Wignall, G. D.; Yang, H. E. *Macromolecules* 1993, 26, 5365.
- (6) Cheung, Y. W.; Stein, R. S.; Wignall, G. D.; Lin, J. S. *Macromolecules* 1994, 27, 2520.
- (7) Cheung, Y. W.; Stein, R. S. In preparation.
- (8) Barham, P. J.; Keller, H. H. *J. Polym. Sci., Phys. Ed.* 1989, 27, 1029.
- (9) Elsner, G.; Koch, M. J.; Bordas, J.; Zachman, H. G. *Makr. Chem.* 1981, 182, 1262.
- (10) Elsner, G.; Riekel, C.; Zachmann, H. G. *Adv. Polym. Sci.* 1985, 67, 1029.
- (11) Nojima, S.; Tsutsui, H.; Urushihara, A. *Polym. J.* 1986, 18, 451.
- (12) Brandrup, J.; Immergut, E. H. *Polymer Handbook*, 2nd ed.; Wiley: New York, 1975.
- (13) Khamatta, F. B.; Warner, F.; Russell, T. P.; Stein, R. S. *J. Polym. Sci., Polym. Phys. Ed.* 1976, 14, 1391.
- (14) Chu, B.; Wu, D. Q.; Howard, R. *Rev. Sci. Instrum.* 1989, 60, 3224.
- (15) Song, H. H.; Stein, R. S.; Wu, D. Q.; Ree, M.; Philips, J. C.; Legrand, A.; Chu, B. *Macromolecules* 1988, 21, 1180.
- (16) Song, H. H.; Wu, D. Q.; Chu, B.; Satkowski, M.; Ree, M.; Stein, R. S.; Philips, J. C. *Macromolecules* 1990, 23, 2380.
- (17) Tashiro, K.; Satkowski, M. M.; Stein, R. S.; Li, Y.; Chu, B.; Hsu, S. L. *Macromolecules* 1992, 25, 1809.
- (18) Glatter, O.; Kratky, O. *Small Angle X-Ray Scattering*; Academic Press: New York, 1982.
- (19) Imai, M.; Mori, K.; Mizukami, T.; Kaji, K.; Kanaya, T. *Polymer* 1992, 33(21) 4457.